18

CT Imaging: Cardiac Electrophysiology Applications

Jerold S. Shinbane and Matthew J. Budoff

Diagnosis and treatment of electrophysiologically related cardiovascular disease requires detailed understanding and characterization of an individual patient's cardiovascular substrate. Cardiac computed tomographic (CT) angiography allows for comprehensive assessment of cardiovascular structure and function through non-invasive simultaneous three-dimensional (3-D) visualization of cardiac chambers, coronary vessels, and thoracic vasculature. This technique enables assessment of structures particularly germane to electrophysiology including: the coronary veins, pulmonary veins, and left atrium (Figure 18.1). Studies can provide identification of ventricular and vascular substrates associated with sudden death and can provide detailed definition of atrial anatomy. In addition to providing substrate identification and characterization, CT angiography can provide relevant roadmaps for catheter ablation, implantable pacemaker and defibrillator placement, intra-procedure correlation with electrophysiologic findings, and follow-up for complications.

In regard to imaging patients with electrophysiologically relevant issues, heart rate and ectopy are important factors. Multidetector CT requires slower ventricular rates (<60–70 beats/minute) during imaging, while electron beam CT can image patients with a greater spectrum of ventricular rates. Ectopy can be problematic with both modalities. In contradistinction to cardiovascular magnetic resonance imaging (CMR), patients with pacemakers and implantable cardiac defibrillators can be studied.

Identification and Characterization of Anatomic Substrates Associated with Sudden Cardiac Death

Sudden cardiac death is associated with a variety of cardiovascular structural and/or electrophysiologic abnormalities, often with the first manifestation of disease being sudden death due to ventricular arrhythmias or non-arrhythmic hemodynamic compromise. Etiologies associated with grossly identifiable anatomic substrates are multiple and include: acute coronary syndromes [1–3], anomalous coronary arteries [4], dilated and ischemic cardiomyopathy [5], hypertrophic cardiomyopathy [6,7], right ventricular dysplasia [8,9], critical aortic stenosis [10], aortic aneurysms [11,12], and complex congenital heart disease [13]. Additional substrates not always associated with gross anatomic abnormalities are primarily diagnosed through electrocardiographic or electrophysiologic evaluation including Wolff–Parkinson–White syndrome [14], long QT syndromes [15], Brugada syndrome [16–18], and significant bradycardia or high-grade atrioventricular block. CT angiographic evaluation can identify anatomic substrates associated with sudden cardiac death and potentially facilitate approaches to therapeutic interventions associated with these diagnoses.

Coronary Artery Disease and Anomalies

Due to the ability to assess the proximal coronary arteries and their relation to the aorta and other thoracic vasculature, anomalous coronary arteries can be diagnosed with CT (Figure 18.2) [19,20]. Anomalous origin of the coronary arteries is a rare cause of sudden cardiac death, with the initial presentation often occurring as sudden death during exertion in a young patient [21,22]. Some anatomies, although anomalous, are not associated with an increased risk of sudden cardiac death. Specific anatomies associated with sudden death risk include takeoff of the left coronary artery from the pulmonary trunk, left coronary artery from the right aortic sinus, and right coronary artery from the left aortic sinus [23].

Significant proximal vessel and left main disease can lead to significant ischemia, ventricular arrhythmias, and hemodynamic collapse with exertion. CT angiography is

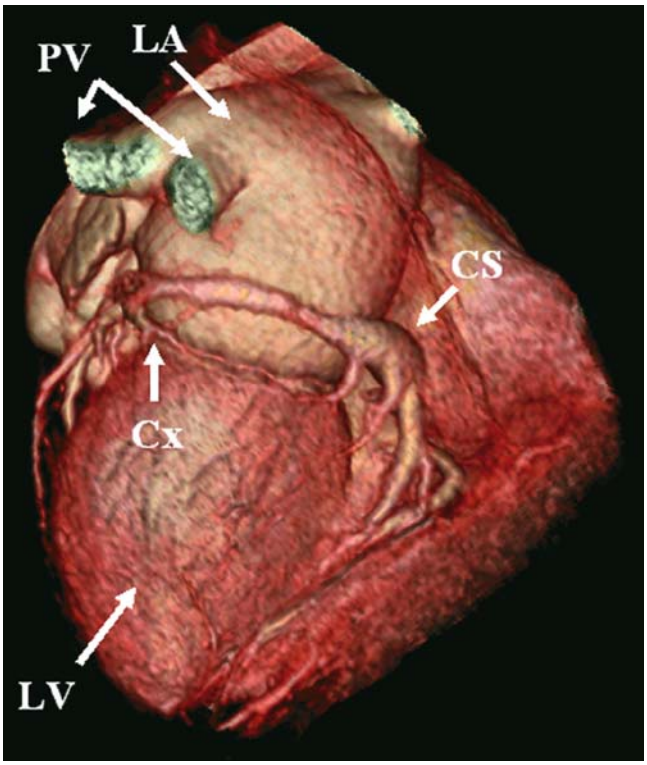

Figure 18.1. CT angiogram with 3-D posterior view demonstrating coronary vasculature including simultaneous imaging of coronary arteries, coronary veins, and their relationships to the left atrium (LA) and left ventricle (LV). CS = coronary sinus, Cx = circumflex, PV = pulmonary vein.

useful for the diagnosis of proximal to mid vessel coronary artery disease [24–34]. Additionally, this technique can assess for patency and stenoses of coronary artery bypass grafts. In regard to electrophysiologic procedures involving induction of ventricular arrhythmias, where left main or left main equivalent disease would be contraindicated, information on proximal coronary artery disease and graft patency may have great relevance.

Sudden death due to plaque rupture and thrombosis often occurs in coronary arterial segments without obstructive disease [1,2]. The focus of cardiac CT has been assessment of plaque burden through calcium scoring. With CT angiography, calcium scoring provides a measure of overall plaque burden, with high Agatston calcium scores (>500) associated with high event rates for myocardial infarction and cardiovascular death, while scores of 0 are associated with extremely low rates of myocardial infarction and cardiovascular death [35]. CT angiography can assess soft plaque, with correlation of findings to intravascular ultrasound, but requires further investigation [36].

Figure 18.2. CT angiography image demonstrating anomalous origin of the left coronary artery off of the pulmonary artery (arrow), which is a substrate associated with sudden cardiac death. PA = pulmonary artery.

Dilated Ischemic and Non-ischemic Cardiomyopathy

Sudden death prevention and treatment in recent years has focused on dilated ischemic and non-ischemic cardiomyopathy with multicenter prospective studies demonstrating benefit to implantable cardiac defibrillator (ICD) therapy when placed solely on anatomic/functional substrate of ischemic cardiomyopathy. The MADIT II study demonstrated a significant decrease in overall mortality with prophylactic ICD placement with criteria for implantation being a substrate of ischemic cardiomyopathy with an ejection fraction of less than or equal to 30% [5]. Recently, data from the Sudden Cardiac Death in Heart Failure Trial have broadened the indications for prophylactic ICD therapy as a primary prevention modality to non-ischemic dilated cardiomyopathy [37]. The results of these studies place particular emphasis on the need for precise quantitative functional assessment of cardiomyopathic substrates, as algorithms for device placement based on these studies allow for implant decisions based on anatomic substrate and ventricular function.

CT angiography can provide detailed assessment of cardiomyopathic cardiac substrates with reproducible quantitative measurement of slice-by-slice volumetric biventricular volumes and ejection fraction, wall thickness, and regional wall motion (Figure 18.3) [38–40]. CT technology helps to differentiate ischemic from non-ischemic dilated cardiomyopathy based on coronary calcium scores [41]. CT angiography can directly visualize coronary arteries, which may potentially facilitate differentiation between ischemic and non-ischemic cardiomyopathy.

In addition to characterization of cardiomyopathy, CT angiography may potentially be useful in facilitation of resynchronization therapy for heart failure in ischemic and non-ischemic dilated cardiomyopathy. In patients with dilated ischemic and non-ischemic cardiomyopathy,

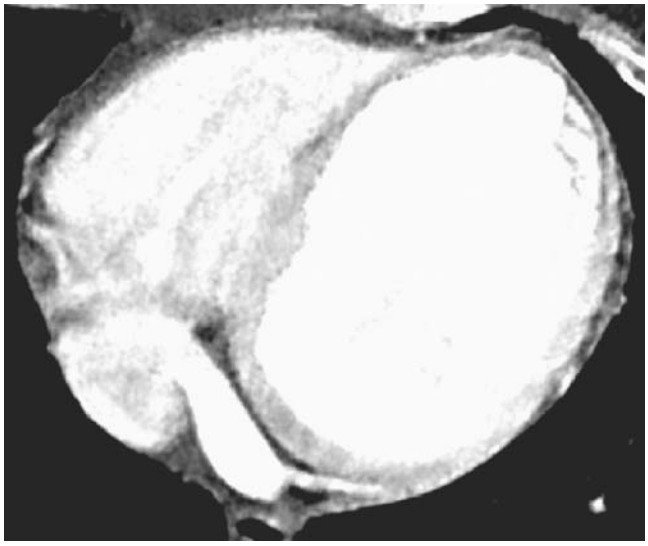

Figure 18.3. Axial slice demonstrating biventricular enlargement in a patient with ischemic cardiomyopathy secondary to previous anterior myocardial infarct. The left ventricular end-diastolic volume was quantified at 179 mL, left ventricular mass at 76 grams, and left ventricular ejection fraction at 35% with anteroapical severe hypokinesis. Thinning of the left ventricular apex is seen.

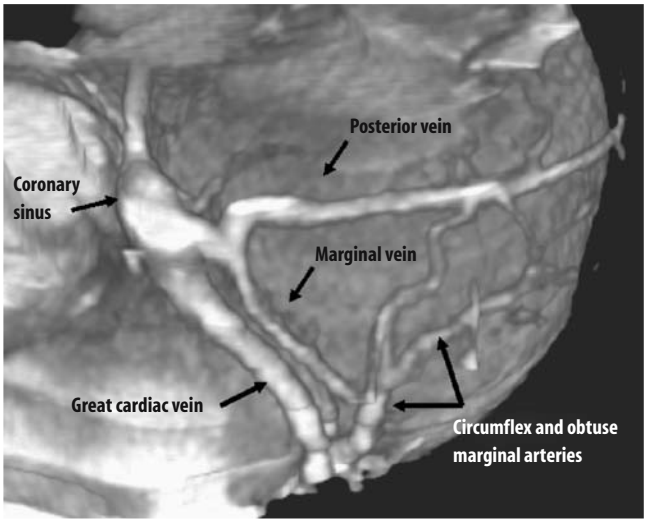

Figure 18.5. CT angiography image demonstrating a coronary branch vein, which subsequently bifurcates into a posterior and marginal branch. The circumflex and obtuse marginal branch arteries are also visualized.

ventricular conduction abnormalities, and moderate to severe heart failure, resynchronization therapy has been shown to decrease heart failure symptoms, improve quality of life, improve ventricular function, and decrease hospitalizations [42–44].

In biventricular pacing, left ventricular pacing is usually achieved via an endocardial approach by placing a chronic pacing lead in a coronary sinus branch vessel (Figure 18.4). Placement of the coronary venous lead can be challenging, as the coronary sinus needs to be cannulated and lead position is limited to the individual location and variation of the existing coronary venous anatomy. CT angiography, due to its ability to visualize coronary veins, can provide detailed assessment of the coronary venous anatomy, with coronary sinus dimensions, branch vessel locations, branch vessel diameters, and branch vessel angulations off of the coronary sinus/great cardiac vein (Figure 18.5) [45–48]. Additionally, 3-D reconstructions can identify specific myocardial segments associated with a particular coronary venous site (Figure 18.6).

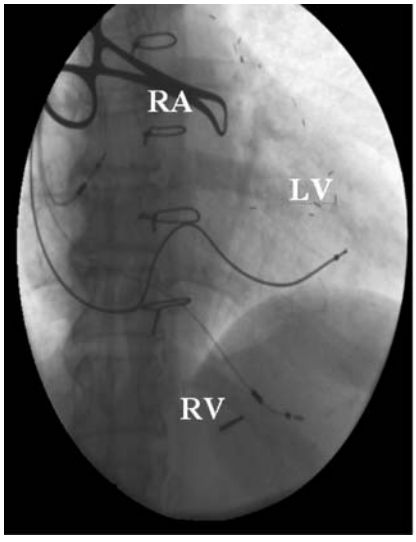

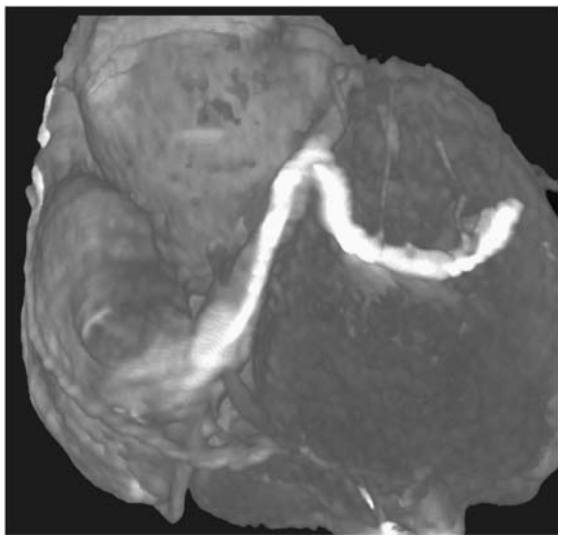

Figure 18.4. Fluoroscopy image demonstrating biventricular pacing leads and CT image demonstrating the position of the coronary sinus lead. RA = right atrial lead, RV = right ventricular lead, and LV = coronary venous lead.

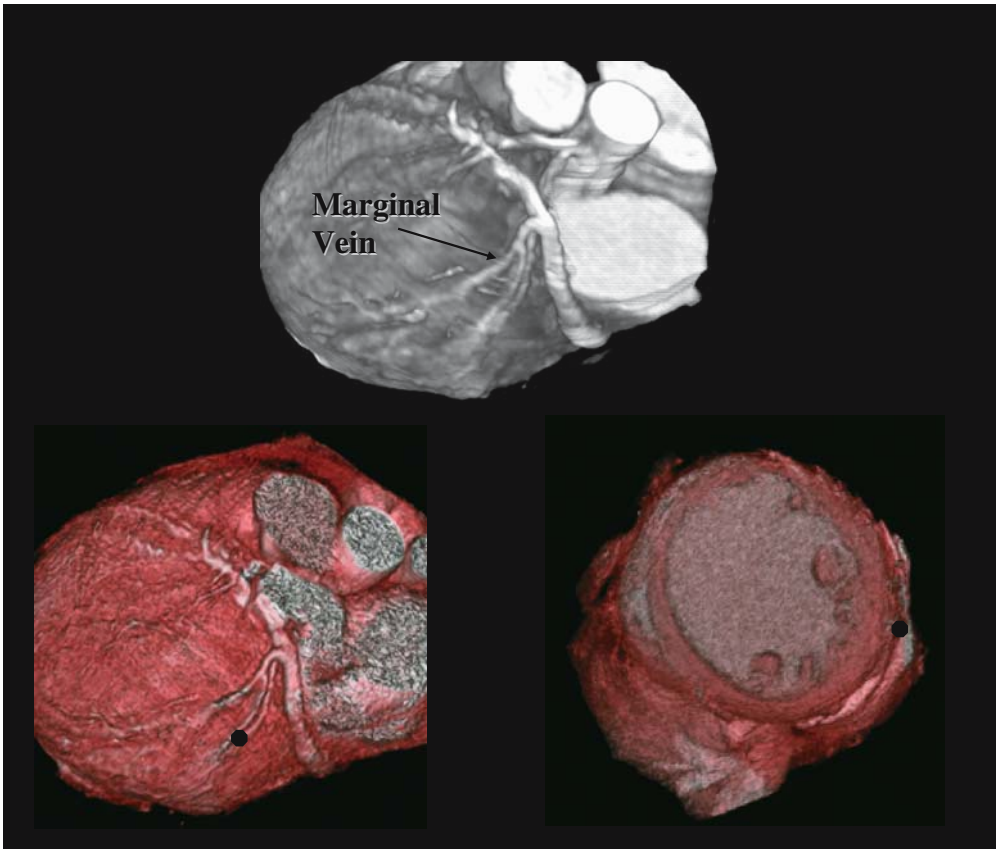

Figure 18.6. CT coronary angiogram demonstrating the coronary venous system (top panel). Three-dimensional localization of the myocardial segment associated with a particular segment of the marginal vein is displayed (black circle, lower panels).

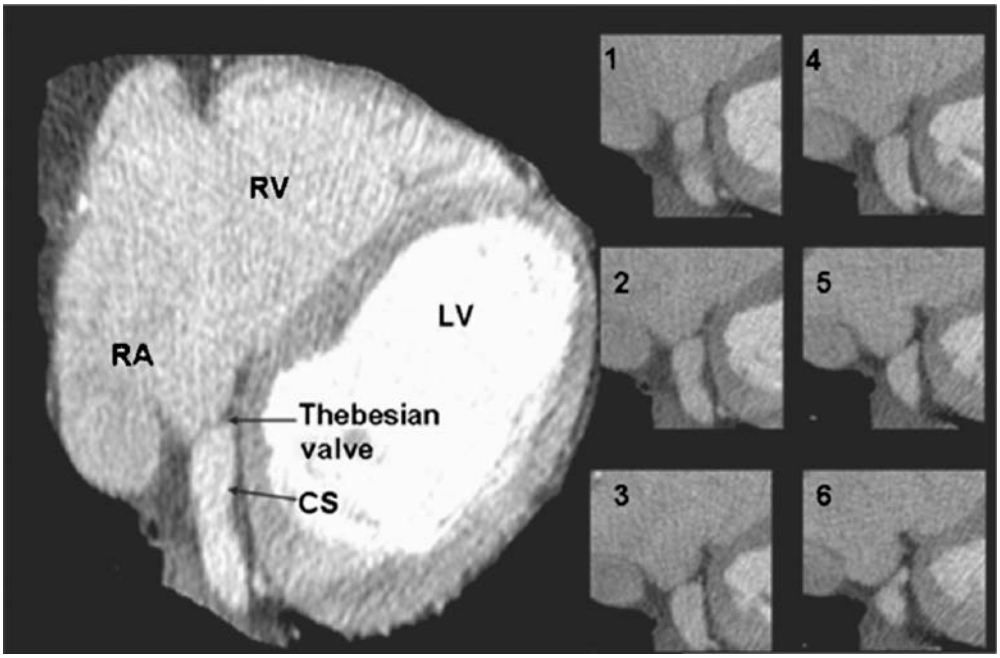

Figure 18.7. Serial CT angiography axial images at the coronary sinus os level, numbered from superior to inferior, demonstrating a prominent Thebesian valve (coronary sinus os valve) on all slices. CS = coronary sinus, RA = right atrium, RV = right ventricle, and LV = left ventricle. (Reprinted from: Shinbane JS, Girsky MJ, Mao S, Budoff MJ. Thebesian valve imaging with electron beam CT angiography: implications for resynchronization therapy. Pacing Clin Electrophysiol 2004;27: 1566–1567, with permission from Blackwell Publishing, USA.)

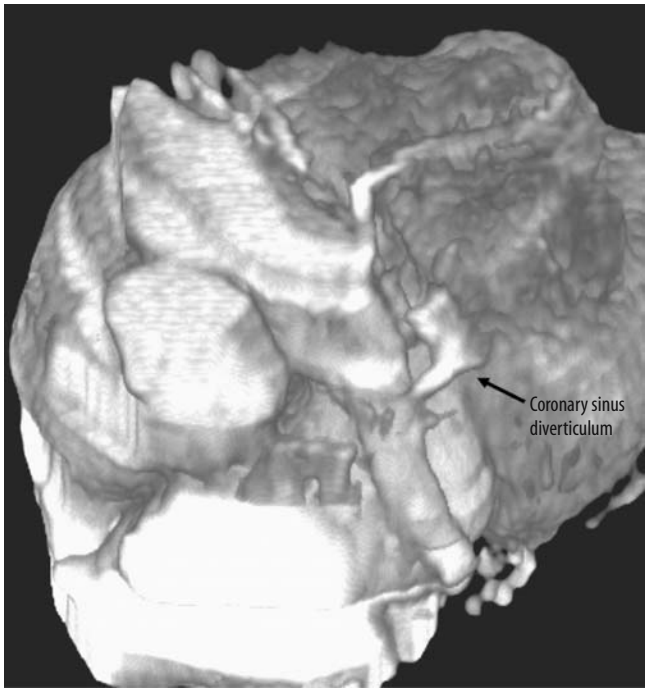

Figure 18.8. CT angiogram demonstrating a coronary sinus diverticulum (arrow).

CT angiography can also visualize details of coronary veins, such as Thebesian valves (prominent coronary vein os valves), which can obstruct access to the coronary sinus (Figure 18.7) [49]. Other abnormalities such as coronary sinus diverticula (Figure 18.8), and anomalous connection such as left superior vena cava to coronary sinus connections (Figure 18.9) can be visualized. The ability to provide venous roadmaps, as well as to assess the spatial relationships between the coronary veins and adjacent cardiac structures, requires further investigation in order to assess its utility in facilitation of coronary venous interventions.

Hypertrophic Cardiomyopathy

Hypertrophic cardiomyopathy can lead to sudden cardiac death due to a variety of mechanisms including atrial and ventricular arrhythmias, bradyarrhythmias, and ischemia [6,50,51]. Echocardiography is the main diagnostic modality for the diagnosis of hypertrophic cardiomyopathy and in addition to anatomy can assess resting and exercise gradients and associated valve function [52,53]. The diagnosis can be also be made by CT angiography with similar left ventricular measures to magnetic resonance imaging, although without hemodynamic gradient data (Figure 18.10) [54].

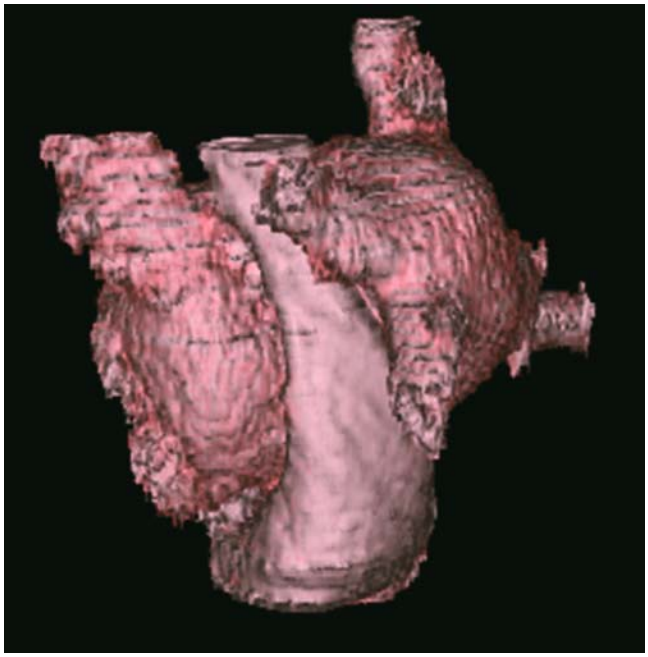

Figure 18.9. Three-dimensional volume-rendered view demonstrating a left superior vena cava with connection to an aneurysmal coronary sinus. A right-sided superior vena cava was not present.

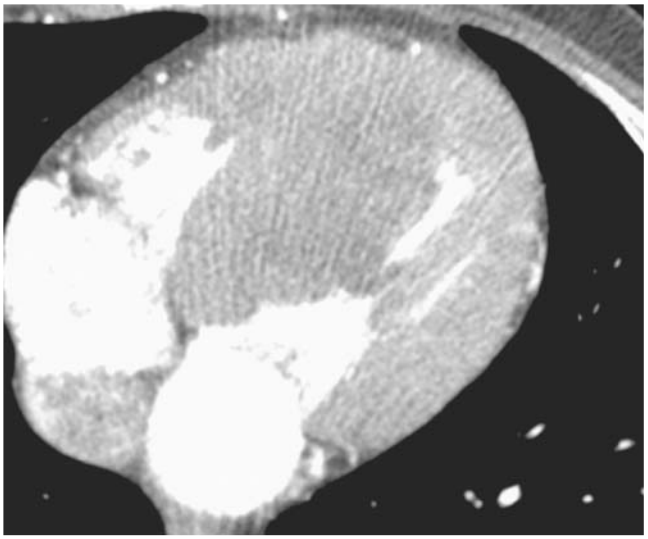

Figure 18.10. CT angiogram demonstrating hypertrophic cardiomyopathy with a profoundly hypertrophied septum.

Right Ventricular Pathology

The diagnosis of right ventricular dysplasia can be challenging, and often the initial presentation is sudden death [8,55]. Imaging is only one component of the diagnosis, which also involves: clinical history of palpitations, syncope or right heart failure symptoms, family history of right ventricular dysplasia or sudden cardiac death from suspected right ventricular dysplasia, ECG criteria, and electrophysiologic testing results [56]. Even with these techniques, the diagnosis can be elusive. Additionally, some right ventricular arrhythmias, such as right ventricular outflow tract tachycardia, are not associated with significant right ventricular pathology and do not confer risk of sudden death. Since similar right ventricular arrhythmias can be associated with either right ventricular dysplasia or right ventricular outflow tract tachycardia, it extremely important to differentiate normal from pathologic right ventricular structure and function.

Cardiovascular magnetic resonance (CMR) is the diagnostic imaging modality of choice for the diagnosis of arrhythmogenic right ventricular dysplasia, due to the ability to differentiate fat and myocardium, as well as the ability to define right ventricular morphology and size, regional wall motion, and ejection fraction. Initial efforts to diagnose right ventricular dysplasia focused on characterization of CMR intramyocardial fat patterns, but there is great variation in these patterns in normal subjects [57,58]. Additionally, CMR findings of myocarditis can mimic arrhythmogenic right ventricular dysplasia [59]. Therefore, diagnosis has focused on right ventricular wall motion abnormalities, right ventricular ejection fraction, and ventricular wall morphologic changes.

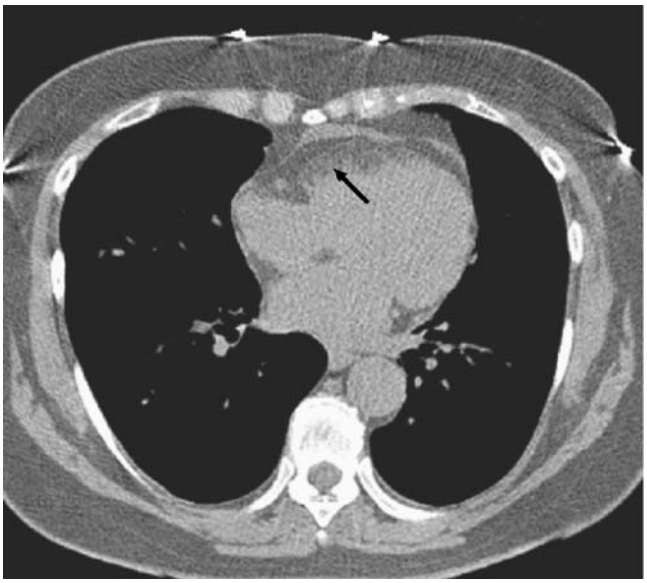

Figure 18.11. CT angiogram demonstrating arrhythmogenic right ventricular dysplasia with fatty replacement of the right ventricular myocardium (arrow).

CT angiography has been assessed for the ability to diagnose anatomic features associated with right ventricular dysplasia, such as epicardial and myocardial fat, low-attenuation trabeculations, and right ventricular free wall scalloping, but has not been evaluated as a screening tool (Figure 18.11) [60–62]. When right ventricular dysplasia is clinically considered as a mechanism of ventricular arrhythmias, comprehensive evaluation with CMR needs to be considered prior to ICD placement, as this modality cannot be used subsequent to device placement. Cardiac CT, although not currently the diagnostic procedure of choice, can be performed when the diagnosis is considered in patients with devices already implanted.

Congenital Heart Disease

A variety of arrhythmic processes are associated with specific congenital anatomies and sudden cardiac death is often associated with worsening of ventricular function late after surgical repair [13]. CT imaging can assess 3-D anatomy and provide comprehensive characterization of native and operated congenital heart disease including ventricular function, myocardial scar, anomalous vascular connections, and shunts [63–65]. Ventricular arrhythmias can be associated with worsening hemodynamic and ventricular function and can also be associated with reentrant circuits involving surgical scars [13]. A spectrum of atrial arrhythmias including atrial tachycardia, a variety of atrial flutter types including incisional reentry in previously operated patients, and atrial fibrillation can occur [66–68]. CT can provide 3-D roadmaps of complex congenital heart disease for pre-procedure planning of surgical or endovascular interventions [63,69].

Aorta and Aortic Valve Pathology

Aortic aneurysm is associated with risk for sudden death due to aortic dissection or rupture associated with connective tissue disorders or acquired cardiovascular disease [70]. CT angiography can diagnose aortic aneurysm, dissection, and wall abnormalities such as penetrating ulcers, calcification or thrombus with ability to assess all aortic segments (Figure 18.12) [71]. From the procedural standpoint, these studies can provide comprehensive assessment for aortic pathology which may affect decisions as to whether a retrograde aortic approach is contraindicated for ablations of left ventricular tachycardias or left-sided accessory pathways.

Severe to critical aortic stenosis can lead to sudden cardiac death and is typically diagnosed by echocardiography. CT can only indirectly assess aortic valve stenosis as aortic valve calcium is a marker for significant aortic valve stenosis. Patients with elevated aortic valve calcium

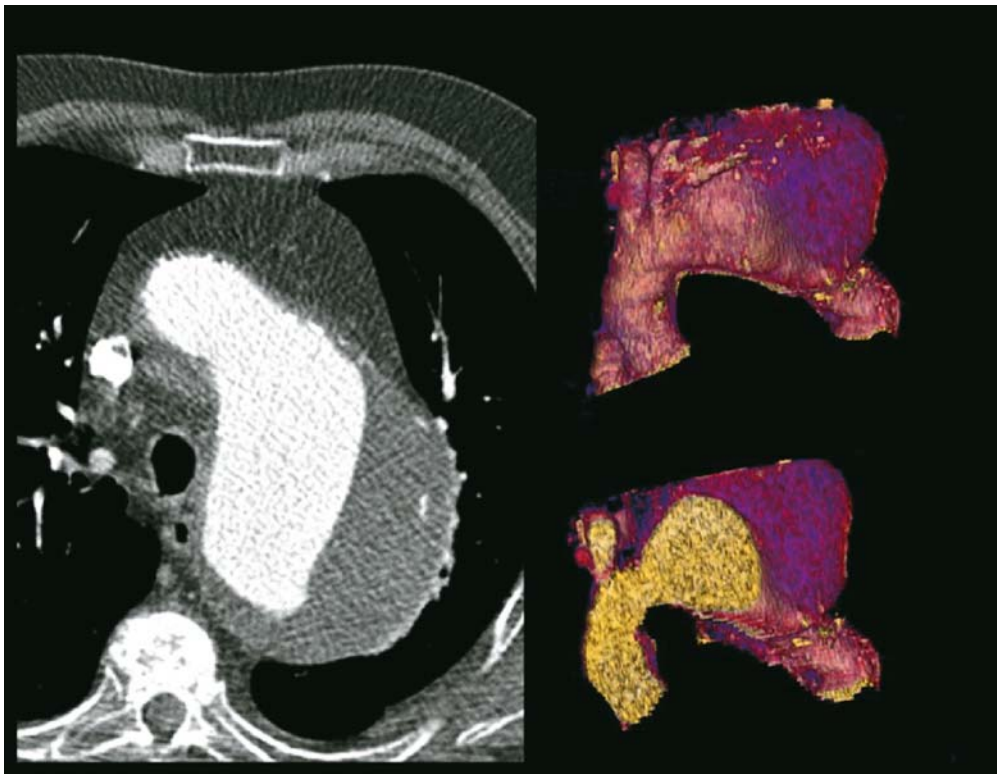

Figure 18.12. Axial 2-D image and 3-D reconstructions demonstrating a large aortic aneurysm with intramural thrombus.

scores should be further assessed for aortic valve disease [72].

Assessment of Atrial Anatomy Associated with Supraventricular Arrhythmias

Cardiac CT angiography can assess atrial anatomy, pulmonary venous anatomy, and coronary venous anatomy, all with great relevance to left atrial arrhythmias including atrial fibrillation, atypical atrial flutter circuits, and focal atrial tachycardias. Catheter-based techniques for ablation of atrial fibrillation have focused on ablation of the pulmonary veins with either segmental ablation or complete circumferential electrical isolation of the pulmonary veins [73–75]. CT imaging can characterize these features through 3-D volume-rendered and endocardial images, including number of veins, location in the atrium, vein size, vein morphology, and vein os complexity (Figures 18.13–18.15) [76]. Preoperative CT angiography can provide a roadmap of atrial and pulmonary vein structure to guide electrophysiologic study and ablation of atrial fibrillation [76,77]. Additionally, integration of 3-D images obtained pre-procedure with real-time catheter position, and electrophysiologic recordings may potentially facilitate ablation procedures [78].

Assessment for atrial thrombi is important to the evaluation, management, and pre-procedure assessment of patients with atrial fibrillation and atrial flutter. CT angiography can visualize the left atrial appendage in detail and has been reported to be able to visualize atrial thrombi [79,80]. Contrast electron beam CT has also been preliminarily compared to transesophageal echocardiography in a series of 96 patients, with detection of all 9 thrombi seen on transesophageal echocardiography studies, although 4 additional false-positive studies were obtained with CT [79]. Further study will be required to assess the utility of CT to rule out atrial thrombus. The ability to assess for atrial thrombus would greatly enhance the comprehensive nature of pre-procedure CT angiography prior to atrial fibrillation ablation.

Pulmonary vein stenosis is a potential complication of atrial fibrillation ablation. The incidence of stenosis has not been completely defined and is dependent on technique and degree of surveillance. CT and MRI have been used to diagnose pulmonary vein stenosis [81–85]. The time course of pulmonary vein stenosis has not been fully defined and long-term studies need to be performed. In addition to significant stenoses, mild to moderate degrees of stenosis can be documented. The long-term possible progression of these stenoses requires further study [86]. Preoperative studies, in addition to providing a roadmap for intervention, can provide templates for follow-up studies assessing for pulmonary vein stenosis.

The 3-D relationship between the left atrium and esophagus may have relevance to atrial fibrillation ablation

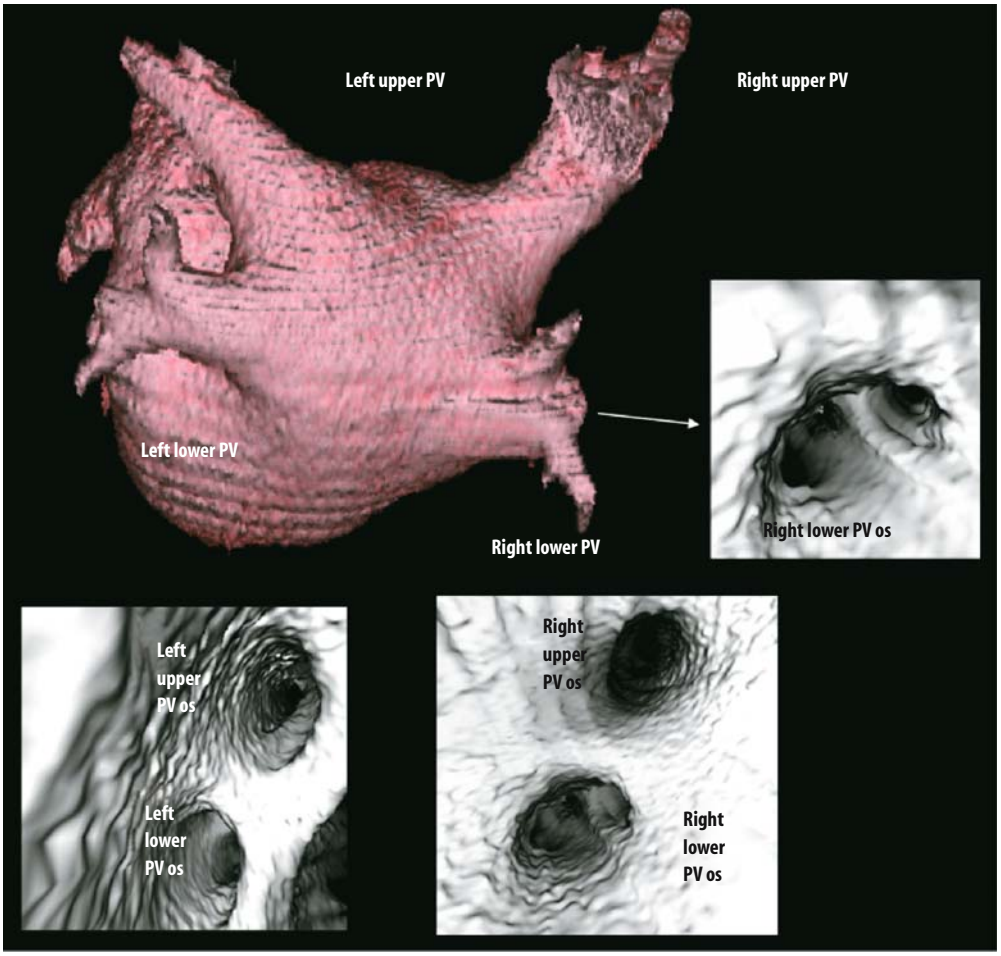

Figure 18.13. Three-D CT angiography volume-rendered view of the posterior left atrium demonstrating the pulmonary veins. Endocardial views demonstrate venous anatomy, relationships between veins, and pulmonary vein os details. PV = pulmonary vein.

approaches, as left atrial-esophageal fistula has been reported as a fatal complication of left atrial ablation for atrial fibrillation [87]. There is variability in the course of the esophagus and degree of contact between the posterior left atrium/pulmonary veins and the esophagus, which can be visualized prior to ablation [88].

As mentioned previously, CT angiography is effective for visualization of the coronary sinus and its tributaries [89]. Coronary sinus anatomy and its relationship to other cardiac structures is important in a variety of supraventricular electrophysiologic procedures, including mapping and ablation of accessory pathways and focal left atrial arrhythmias [90–92]. Coronary sinus anatomy is important in ablation of posteroseptal accessory pathways, as these pathways are often associated with coronary sinus diverticula with successful ablation often performed in the coronary sinus diverticulum. CT angiography can visualize coronary sinus diverticula (Figure 18.8). Additionally, understanding the relationship of coronary veins, coronary arteries, and myocardium may be important if ablation in a coronary vein is considered in order to avoid coronary artery complications, especially if a coronary artery courses between the coronary vein and epicardium. CT angiography can define these relationships including the relationship between the circumflex coronary artery and coronary sinus/great cardiac vein (Figures 18.16–18.18) [47,48].

Congenital anomalies affecting the atria such as atrial septal defect, [93,94] and Ebstein anomaly [95], which can be associated with accessory pathways, can be

Figure 18.14. **a** CT angiography 3-D volume-rendered image of the left atrium demonstrating the spatial relationships between the pulmonary veins, atrial appendage, and atrium on a posterior view. There is a small additional pulmonary vein near the os of the right lower pulmonary vein. PV = pulmonary vein. **b** Endocardial image demonstrating left atrial endocardial anatomy with spatial relationship between the right upper and right lower pulmonary vein. The small additional os near the right lower pulmonary vein is also visualized. **c** Endocardial image demonstrating left atrial endocardial anatomy with spatial relationship between the left upper and left lower pulmonary vein, as well as the relationship between the left upper pulmonary vein and the left atrial appendage. A closer view better defines the muscular ridge between the left upper and left lower pulmonary veins. **d** Axial 2-D images of the left upper, left lower, right upper, and right lower pulmonary veins, and an additional vein near the right lower pulmonary vein. These images are helpful for quantitation of pulmonary vein size, and understanding of these images is enhanced through reference to the 3-D images. (**a** and **b** reprinted from: Shinbane JS, Girsky MJ, Chau A, Mao S, Budoff MJ. Three-dimensional computed tomography imaging of left atrial anatomy for atrial fibrillation ablation. Clin Cardiol 2005;28:100, with permission from Clinical Cardiology Publishing Company, Inc., Mahwah, NJ, USA.)

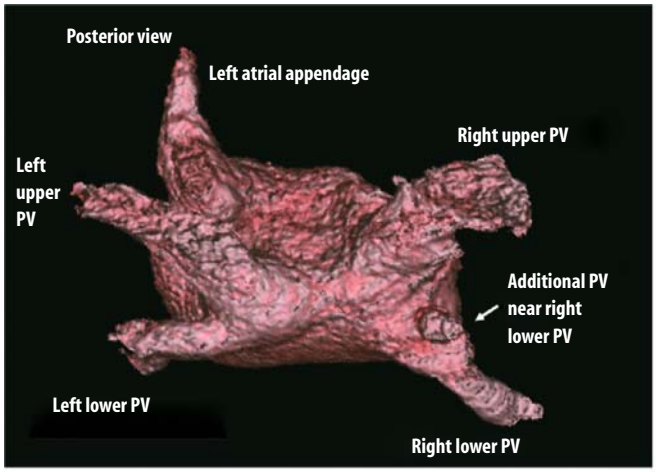
Posterior view
Left atrial appendage
Right upper PV
Left upper PV
Additional PV near right lower PV
Left lower PV
Right lower PV

a

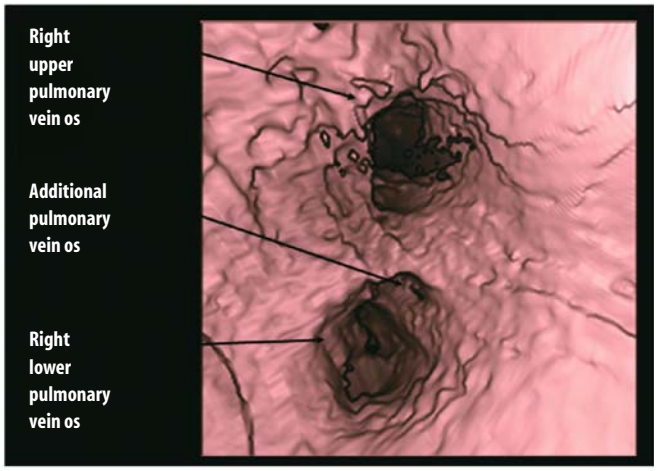
Right upper pulmonary vein os
Additional pulmonary vein os
Right lower pulmonary vein os

b

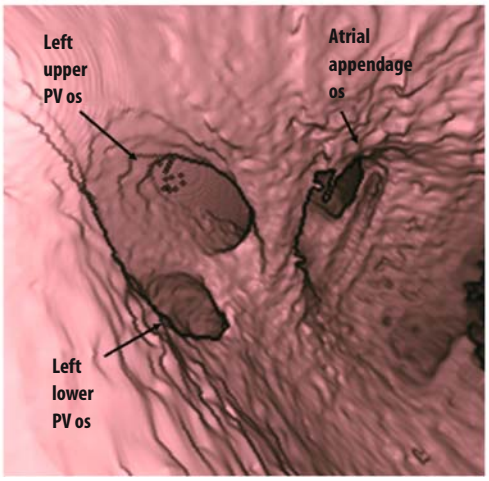
Left upper PV os
Atrial appendage os
Left lower PV os

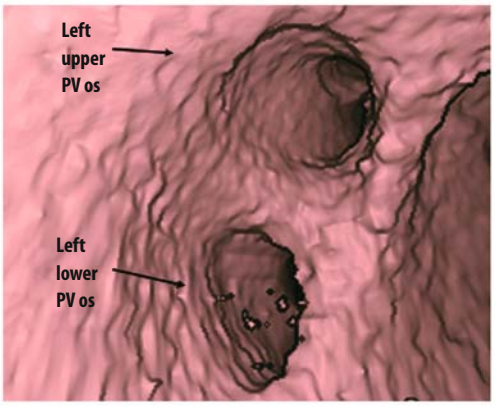
Left upper PV os
Left lower PV os

c

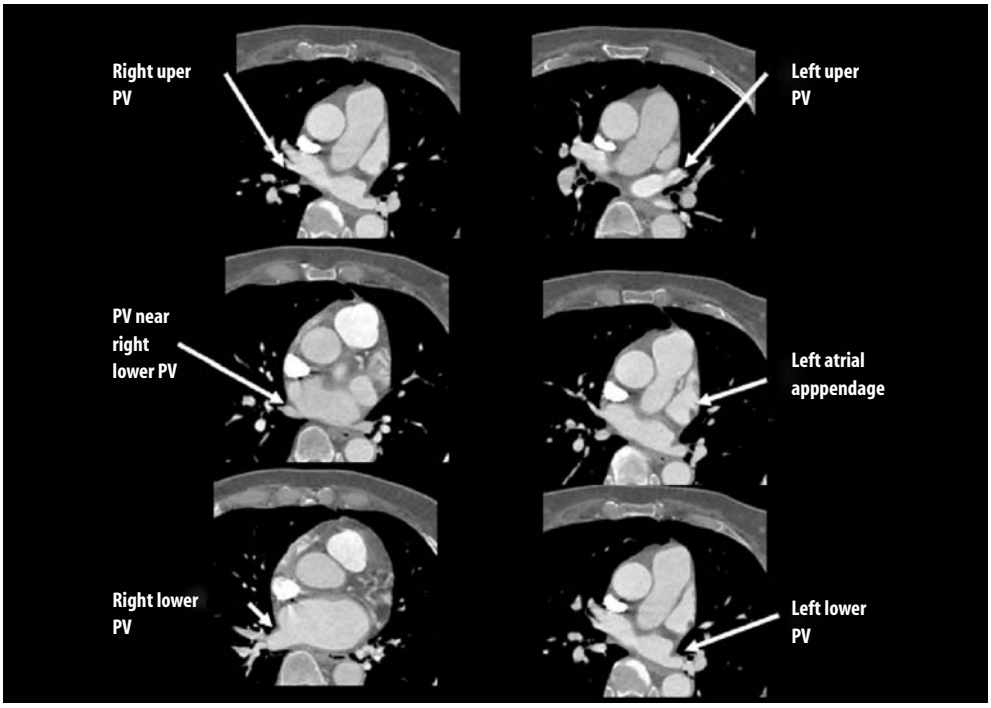
Right uper PV
Left uper PV
PV near right lower PV
Left atrial apppendage
Right lower PV
Left lower PV

d

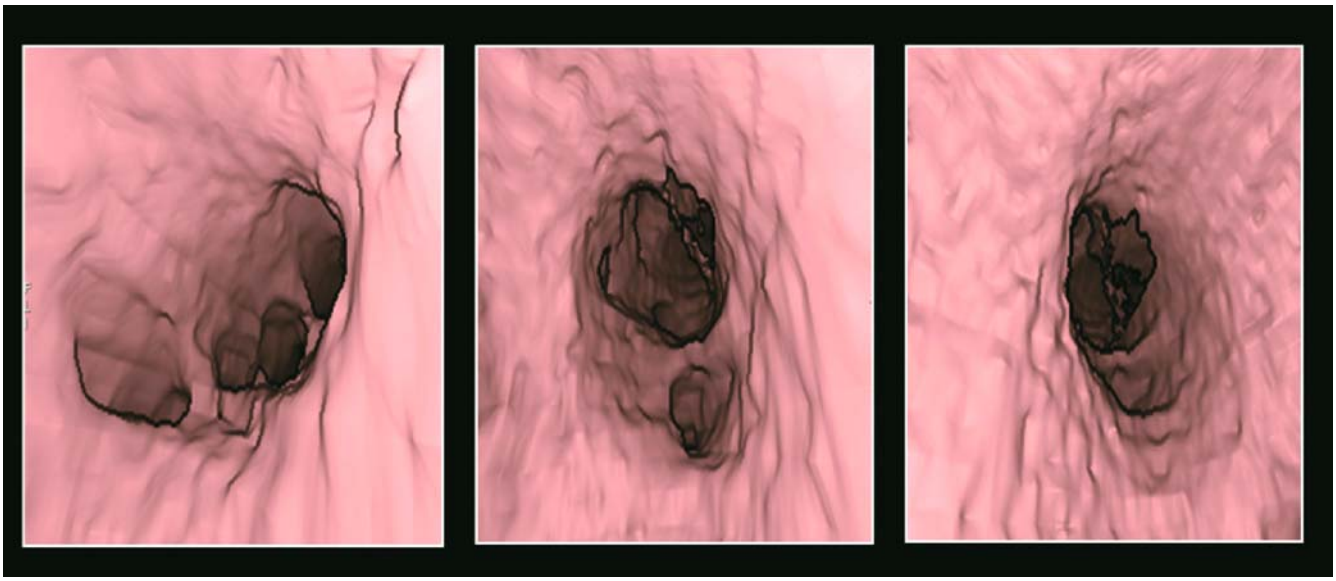

Figure 18.15. Endocardial views of pulmonary veins demonstrating variation in the complexity of the pulmonary vein os.

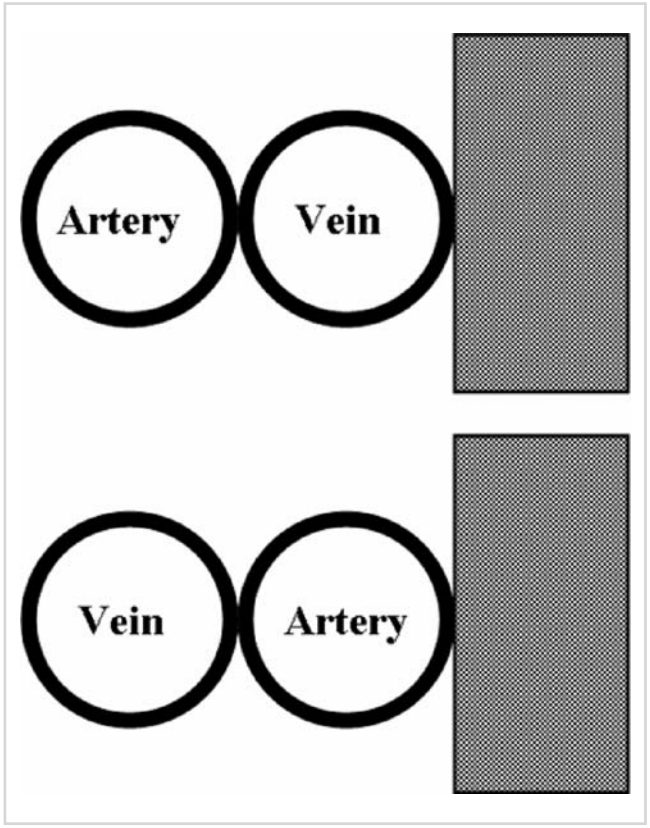

Figure 18.16. Schematic diagram of 3-D spatial arrangements between the coronary arteries and coronary veins in overlapping segments in reference to the epicardium. The medial vessel is the vessel closer to epicardium in overlapping segments.

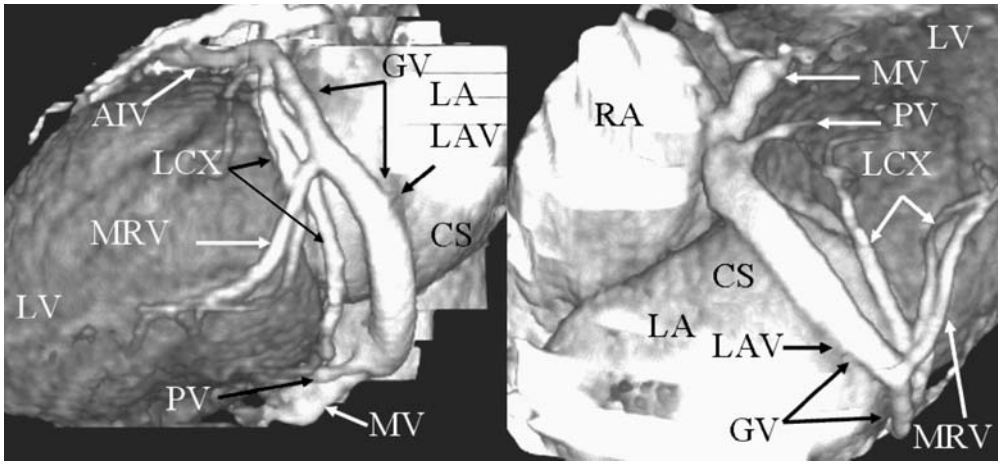

Figure 18.17. The left-lateral view (left panel) and diaphragmatic view (right panel) of the heart. The left circumflex coronary artery and coronary veins are clearly displayed. The great cardiac vein is seen overlying the left circumflex coronary artery for a short (<30 mm) segment. The marginal vein is dominant and the posterior vein is small in size. AIV = anterior interventricular vein, CS = coronary sinus, GV = great cardiac vein, LA = left atrium, LAV = left atrial vein, LCX = left circumflex coronary artery, LV = left ventricle, MV = middle cardiac vein, MRV = marginal vein, PV = posterior vein. (Reprinted from: Mao S, Shinbane JS, Girsky MJ, Child J, Carson S, Flores F, Oudiz RJ, Budoff MJ. Three-dimensional coronary venous imaging with computed tomographic angiography. Am Heart J 2005;150:315–322, with permission of Elsevier, Philadelphia, PA, USA.)

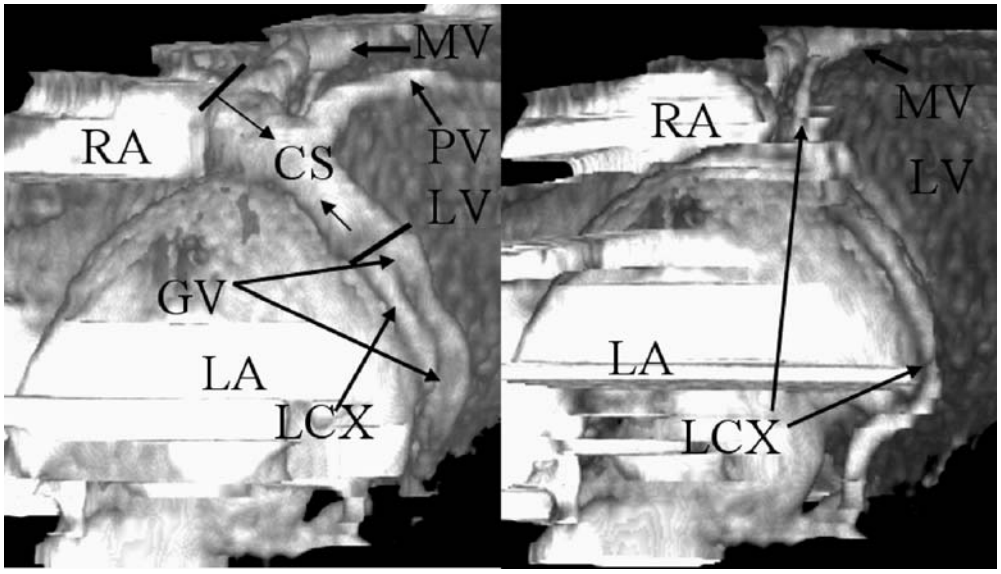

Figure 18.18. The relationship between the circumflex coronary artery and coronary sinus/great cardiac vein is displayed. The great cardiac vein is lateral and covering the circumflex for almost the entire circumflex course. After editing the 3-D images to remove the coronary sinus/great cardiac vein, the circumflex is displayed. The coronary sinus boundary is clear and the coronary sinus distance is marked between arrows (→ ←). The posterior vein is dominant and marginal vein is not present. CS = coronary sinus, GV = great cardiac vein, MV = middle vein, MRV = marginal vein, PV = posterior vein, LA = left atrium, LAV = left atrial vein, LCx = left circumflex coronary artery, LV = left ventricle, and RA = right atrium. (Reprinted from: Mao S, Shinbane JS, Girsky MJ, Child J, Carson S, Flores F, Oudiz RJ, Budoff MJ. Three-dimensional coronary venous imaging with computed tomographic angiography. Am Heart J 2005; In press, with permission of Elsevier, Philadelphia, PA, USA.)

characterized by CT angiography. Anomalous venous return to the atria such as persistent left superior vena cava often with connection to the coronary sinus can be imaged and has great relevance to the approach to placement of pacemakers and ICDs (Figure 18.9) [96].

Summary

The ability of CT angiography to comprehensively assess cardiovascular structure and function makes it a robust technology for the assessment, treatment, and follow-up of patients with electrophysiologically related disease processes. Cardiovascular CT angiographic imaging holds the promise to continue to advance the field of cardiac electrophysiology through understanding of electrophysiologically relevant pathologic substrates and facilitation of novel interventional approaches. This effort will be enhanced by a multidisciplinary approach to diagnosis and therapeutic intervention in patients with electrophysiologically relevant issues.

References

1. Naghavi M, Libby P, Falk E, et al. From vulnerable plaque to vulnerable patient: a call for new definitions and risk assessment strategies: Part I. Circulation 2003;108:1664–1672.

2. Naghavi M, Libby P, Falk E, et al. From vulnerable plaque to vulnerable patient: a call for new definitions and risk assessment strategies: Part II. Circulation 2003;108:1772–1778.
3. Burke AP, Farb A, Malcom GT, Liang Y, Smialek JE, Virmani R. Plaque rupture and sudden death related to exertion in men with coronary artery disease. JAMA 1999;281:921–926.
4. Basso C, Corrado D, Thiene G. Congenital coronary artery anomalies as an important cause of sudden death in the young. Cardiol Rev 2001;9:312–317.
5. Moss AJ, Zareba W, Hall WJ, et al. Prophylactic implantation of a defibrillator in patients with myocardial infarction and reduced ejection fraction. N Engl J Med 2002;346:877–883.
6. Elliott PM, Poloniecki J, Dickie S, et al. Sudden death in hypertrophic cardiomyopathy: identification of high risk patients. J Am Coll Cardiol 2000;36:2212–2218.
7. Maron BJ. Hypertrophic cardiomyopathy: a systematic review. JAMA 2002;287:1308–1320.
8. Corrado D, Thiene G, Nava A, Rossi L, Pennelli N. Sudden death in young competitive athletes: clinicopathologic correlations in 22 cases. Am J Med 1990;89:588–596.
9. Corrado D, Basso C, Thiene G, et al. Spectrum of clinicopathologic manifestations of arrhythmogenic right ventricular cardiomyopathy/dysplasia: a multicenter study. J Am Coll Cardiol 1997;30:1512–1520.
10. Wolfe RR, Driscoll DJ, Gersony WM, et al. Arrhythmias in patients with valvar aortic stenosis, valvar pulmonary stenosis, and ventricular septal defect. Results of 24-hour ECG monitoring. Circulation 1993;87:I89–101.
11. Fikar CR, Koch S. Etiologic factors of acute aortic dissection in children and young adults. Clin Pediatr (Phila) 2000;39:71–80.
12. Glorioso J Jr, Reeves M. Marfan syndrome: screening for sudden death in athletes. Curr Sports Med Rep 2002;1:67–74.
13. Ghai A, Silversides C, Harris L, Webb GD, Siu SC, Therrien J. Left ventricular dysfunction is a risk factor for sudden cardiac death in adults late after repair of tetralogy of Fallot. J Am Coll Cardiol 2002; 40:1675–1680.
14. Sharma AD, Yee R, Guiraudon G, Klein GJ. Sensitivity and specificity of invasive and noninvasive testing for risk of sudden death in Wolff–Parkinson–White syndrome. J Am Coll Cardiol 1987;10:373–381.
15. Towbin JA. Molecular genetic basis of sudden cardiac death. Cardiovasc Pathol 2001;10:283–295.
16. Brugada P, Brugada J. Right bundle branch block, persistent ST segment elevation and sudden cardiac death: a distinct clinical and electrocardiographic syndrome. A multicenter report. J Am Coll Cardiol 1992;20:1391–1396.
17. Brugada J, Brugada P, Brugada R. The syndrome of right bundle branch block ST segment elevation in V1 to V3 and sudden death – the Brugada syndrome. Europace 1999;1:156–166.
18. Antzelevitch C, Brugada P, Brugada J, Brugada R, Towbin JA, Nademanee K. Brugada syndrome: 1992–2002: a historical perspective. J Am Coll Cardiol 2003;41:1665–1671.
19. Ropers D, Moshage W, Daniel WG, Jessl J, Gottwik M, Achenbach S. Visualization of coronary artery anomalies and their anatomic course by contrast-enhanced electron beam tomography and three-dimensional reconstruction. Am J Cardiol 2001;87:193–197.
20. Van Ooijen PM, Dorgelo J, Zijlstra F, Oudkerk M. Detection, visualization and evaluation of anomalous coronary anatomy on 16-slice multidetector-row CT. Eur Radiol 2004;14(12):2163–2171.
21. Basso C, Maron BJ, Corrado D, Thiene G. Clinical profile of congenital coronary artery anomalies with origin from the wrong aortic sinus leading to sudden death in young competitive athletes. J Am Coll Cardiol 2000;35:1493–1501.
22. Maron BJ, Shirani J, Poliac LC, Mathenge R, Roberts WC, Mueller FO. Sudden death in young competitive athletes. Clinical, demographic, and pathological profiles. JAMA 1996;276:199–204.
23. Frescura C, Basso C, Thiene G, et al. Anomalous origin of coronary arteries and risk of sudden death: a study based on an autopsy population of congenital heart disease. Hum Pathol 1998;29:689–695.
24. Moshage WE, Achenbach S, Seese B, Bachmann K, Kirchgeorg M. Coronary artery stenoses: three-dimensional imaging with electrocardiographically triggered, contrast agent-enhanced, electron-beam CT. Radiology 1995;196:707–714.
25. Schmermund A, Rensing BJ, Sheedy PF, Bell MR, Rumberger JA. Intravenous electron-beam computed tomographic coronary angiography for segmental analysis of coronary artery stenoses. J Am Coll Cardiol 1998;31:1547–1554.
26. Reddy GP, Chernoff DM, Adams JR, Higgins CB. Coronary artery stenoses: assessment with contrast-enhanced electron-beam CT and axial reconstructions. Radiology 1998;208:167–172.
27. Achenbach S, Moshage W, Ropers D, Nossen J, Daniel WG. Value of electron-beam computed tomography for the noninvasive detection of high-grade coronary-artery stenoses and occlusions. N Engl J Med 1998;339:1964–1971.
28. Budoff MJ, Oudiz RJ, Zalace CP, et al. Intravenous three-dimensional coronary angiography using contrast enhanced electron beam computed tomography. Am J Cardiol 1999;83:840–845.
29. Achenbach S, Ropers D, Regenfus M, Muschiol G, Daniel WG, Moshage W. Contrast enhanced electron beam computed tomography to analyse the coronary arteries in patients after acute myocardial infarction. Heart 2000;84:489–493.
30. Lu B, Shavelle DM, Mao S, et al. Improved accuracy of noninvasive electron beam coronary angiography. Invest Radiol 2004;39:73–79.
31. Budoff MJ, Lu B, Shinbane JS, et al. Methodology for improved detection of coronary stenoses with computed tomographic angiography. Am Heart J 2004;148:1085–1090.
32. Nieman K, Cademartiri F, Lemos PA, Raaijmakers R, Pattynama PM, de Feyter PJ. Reliable noninvasive coronary angiography with fast submillimeter multislice spiral computed tomography. Circulation 2002;106:2051–2054.
33. Ropers D, Baum U, Pohle K, et al. Detection of coronary artery stenoses with thin-slice multi-detector row spiral computed tomography and multiplanar reconstruction. Circulation 2003;107:664–666.
34. Budoff MJ, Achenbach S, Duerinckx A. Clinical utility of computed tomography and magnetic resonance techniques for noninvasive coronary angiography. J Am Coll Cardiol 2003;42:1867–1878.
35. Georgiou D, Budoff MJ, Kaufer E, Kennedy JM, Lu B, Brundage BH. Screening patients with chest pain in the emergency department using electron beam tomography: a follow-up study. J Am Coll Cardiol 2001;38:105–110.
36. Achenbach S, Moselewski F, Ropers D, et al. Detection of calcified and noncalcified coronary atherosclerotic plaque by contrast-enhanced, submillimeter multidetector spiral computed tomography: a segment-based comparison with intravascular ultrasound. Circulation 2004;109:14–17.
37. Bardy GH, Lee KL, Mark DB, et al. Amiodarone or an implantable cardioverter-defibrillator for congestive heart failure. N Engl J Med 2005;352:225–237.
38. Rich S, Chomka EV, Stagl R, Shanes JG, Kondos GT, Brundage BH. Determination of left ventricular ejection fraction using ultrafast computed tomography. Am Heart J 1986;112:392–396.
39. Rumberger JA, Behrenbeck T, Bell MR, et al. Determination of ventricular ejection fraction: a comparison of available imaging methods. The Cardiovascular Imaging Working Group. Mayo Clin Proc 1997;72:860–870.
40. Schmermund A, Rensing BJ, Sheedy PF, Rumberger JA. Reproducibility of right and left ventricular volume measurements by electron-beam CT in patients with congestive heart failure. Int J Card Imaging 1998;14:201–209.
41. Budoff MJ, Shavelle DM, Lamont DH, et al. Usefulness of electron beam computed tomography scanning for distinguishing ischemic from nonischemic cardiomyopathy. J Am Coll Cardiol 1998;32: 1173–1178.

42. Abraham WT, Fisher WG, Smith AL, et al. Cardiac resynchronization in chronic heart failure. N Engl J Med 2002;346:1845–1853.
43. Saxon LA, De Marco T, Schafer J, Chatterjee K, Kumar UN, Foster E. Effects of long-term biventricular stimulation for resynchronization on echocardiographic measures of remodeling. Circulation 2002; 105:1304–1310.
44. St John Sutton MG, Plappert T, Abraham WT, et al. Effect of cardiac resynchronization therapy on left ventricular size and function in chronic heart failure. Circulation 2003;107:1985–1990.
45. Gerber TC, Sheedy PF, Bell MR, et al. Evaluation of the coronary venous system using electron beam computed tomography. Int J Cardiovasc Imaging 2001;17:65–75.
46. Girsky MJ, Mao S, Shinbane JS, et al. Electron beam computed tomographic angiography: Three-dimensional characterization of anatomy for coronary vein intervention. Heart Rhythm 2004;1:S26 Abstract.
47. Shinbane JS, Mao S, Girsky MJ, et al. Computed tomographic angiography can define three-dimensional relationships between coronary veins and coronary arteries relevant to coronary venous procedures. Circulation 2004;110:702.
48. Mao S, Shinbane JS, Girsky MJ, et al. Three-dimensional coronary venous imaging with computed tomographic angiography. Am Heart J 2005;150:315–322.
49. Shinbane JS, Girsky MJ, Mao S, Budoff MJ. Thebesian valve imaging with electron beam CT angiography: implications for resynchronization therapy. Pacing Clin Electrophysiol 2004;27:1566–1567.
50. Maron BJ, Shen WK, Link MS, et al. Efficacy of implantable cardioverter-defibrillators for the prevention of sudden death in patients with hypertrophic cardiomyopathy. N Engl J Med 2000; 342:365–373.
51. Maron MS, Olivotto I, Betocchi S, et al. Effect of left ventricular outflow tract obstruction on clinical outcome in hypertrophic cardiomyopathy. N Engl J Med 2003;348:295–303.
52. Klues HG, Schiffers A, Maron BJ. Phenotypic spectrum and patterns of left ventricular hypertrophy in hypertrophic cardiomyopathy: morphologic observations and significance as assessed by two-dimensional echocardiography in 600 patients. J Am Coll Cardiol 1995;26:1699–1708.
53. Charron P, Dubourg O, Desnos M, et al. Diagnostic value of electrocardiography and echocardiography for familial hypertrophic cardiomyopathy in a genotyped adult population. Circulation 1997;96: 214–219.
54. Stone DL, Petch MC, Verney GI, Dixon AK. Computed tomography in patients with hypertrophic cardiomyopathy. Br Heart J 1984;52: 136–139.
55. Tabib A, Loire R, Chalabreysse L, et al. Circumstances of death and gross and microscopic observations in a series of 200 cases of sudden death associated with arrhythmogenic right ventricular cardiomyopathy and/or dysplasia. Circulation 2003;108:3000–3005.
56. Wilde AA, Antzelevitch C, Borggrefe M, et al. Proposed diagnostic criteria for the Brugada syndrome: consensus report. Circulation 2002;106:2514–2519.
57. Tandri H, Calkins H, Nasir K, et al. Magnetic resonance imaging findings in patients meeting task force criteria for arrhythmogenic right ventricular dysplasia. J Cardiovasc Electrophysiol 2003;14:476–482.
58. di Cesare E. MRI assessment of right ventricular dysplasia. Eur Radiol 2003;13:1387–1393.
59. Chimenti C, Pieroni M, Maseri A, Frustaci A. Histologic findings in patients with clinical and instrumental diagnosis of sporadic arrhythmogenic right ventricular dysplasia. J Am Coll Cardiol 2004;43:2305–2313.
60. Dery R, Lipton MJ, Garrett JS, Abbott J, Higgins CB, Schienman MM. Cine-computed tomography of arrhythmogenic right ventricular dysplasia. J Comput Assist Tomogr 1986;10:120–123.
61. Hamada S, Takamiya M, Ohe T, Ueda H. Arrhythmogenic right ventricular dysplasia: evaluation with electron-beam CT. Radiology 1993;187:723–727.
62. Tada H, Shimizu W, Ohe T, et al. Usefulness of electron-beam computed tomography in arrhythmogenic right ventricular dysplasia. Relationship to electrophysiological abnormalities and left ventricular involvement. Circulation 1996;94:437–444.
63. Chen SJ, Li YW, Wang JK, et al. Three-dimensional reconstruction of abnormal ventriculoarterial relationship by electron beam CT. J Comput Assist Tomogr 1998;22:560–568.
64. Chen SJ, Wang JK, Li YW, Chiu IS, Su CT, Lue HC. Validation of pulmonary venous obstruction by electron beam computed tomography in children with congenital heart disease. Am J Cardiol 2001; 87:589–593.
65. Choe KO, Hong YK, Kim HJ, et al. The use of high-resolution computed tomography in the evaluation of pulmonary hemodynamics in patients with congenital heart disease: in pulmonary vessels larger than 1 mm in diameter. Pediatr Cardiol 2000;21:202–210.
66. Cosio FG, Martin-Penato A, Pastor A, Nunez A, Goicolea A. Atypical flutter: a review. Pacing Clin Electrophysiol 2003;26:2157–2169.
67. Balaji S, Harris L. Atrial arrhythmias in congenital heart disease. Cardiol Clin 2002;20:459–468, vii.
68. Kirsh JA, Walsh EP, Triedman JK. Prevalence of and risk factors for atrial fibrillation and intra-atrial reentrant tachycardia among patients with congenital heart disease. Am J Cardiol 2002;90:338–340.
69. Haramati LB, Glickstein JS, Issenberg HJ, Haramati N, Crooke GA. MR imaging and CT of vascular anomalies and connections in patients with congenital heart disease: significance in surgical planning. Radiographics 2002;22:337–347; discussion 348–349.
70. Lu B, Dai RP, Jing BL, et al. Electron beam tomography with three-dimensional reconstruction in the diagnosis of aortic diseases. J Cardiovasc Surg (Torino) 2000;41:659–668.
71. Hartnell GG. Imaging of aortic aneurysms and dissection: CT and MRI. J Thorac Imaging 2001;16:35–46.
72. Shavelle DM, Budoff MJ, Buljubasic N, et al. Usefulness of aortic valve calcium scores by electron beam computed tomography as a marker for aortic stenosis. Am J Cardiol 2003;92:349–353.
73. Nakagawa H, Aoyama H, Beckman KJ, et al. Relation between pulmonary vein firing and extent of left atrial-pulmonary vein connection in patients with atrial fibrillation. Circulation 2004;109:1523–1529.
74. Pappone C, Rosanio S, Oreto G, et al. Circumferential radiofrequency ablation of pulmonary vein ostia: A new anatomic approach for curing atrial fibrillation. Circulation 2000;102:2619–2628.
75. Oral H, Knight BP, Ozaydin M, et al. Segmental ostial ablation to isolate the pulmonary veins during atrial fibrillation: feasibility and mechanistic insights. Circulation 2002;106:1256–1262.
76. Scharf C, Sneider M, Case I, et al. Anatomy of the pulmonary veins in patients with atrial fibrillation and effects of segmental ostial ablation analyzed by computed tomography. J Cardiovasc Electrophysiol 2003;14:150–155.
77. Kato R, Lickfett L, Meininger G, et al. Pulmonary vein anatomy in patients undergoing catheter ablation of atrial fibrillation: lessons learned by use of magnetic resonance imaging. Circulation 2003; 107:2004–2010.
78. Solomon SB, Dickfeld T, Calkins H. Real-time cardiac catheter navigation on three-dimensional CT images. J Interv Card Electrophysiol 2003;8:27–36.
79. Tani T, Yamakami S, Matsushita T, et al. Usefulness of electron beam tomography in the prone position for detecting atrial thrombi in chronic atrial fibrillation. J Comput Assist Tomogr 2003;27:78–84.
80. Alam G, Addo F, Malik M, Levinsky R, Lieb D. Detection of left atrial appendage thrombus by spiral CT scan. Echocardiography 2003;20:99–100.
81. Robbins IM, Colvin EV, Doyle TP, et al. Pulmonary vein stenosis after catheter ablation of atrial fibrillation. Circulation 1998;98:1769–1775.
82. Taylor GW, Kay GN, Zheng X, Bishop S, Ideker RE. Pathological effects of extensive radiofrequency energy applications in the pulmonary veins in dogs. Circulation 2000;101:1736–1742.

83. Yang M, Akbari H, Reddy GP, Higgins CB. Identification of pulmonary vein stenosis after radiofrequency ablation for atrial fibrillation using MRI. J Comput Assist Tomogr 2001;25:34–35.
84. Qureshi AM, Prieto LR, Latson LA, et al. Transcatheter angioplasty for acquired pulmonary vein stenosis after radiofrequency ablation. Circulation 2003;108:1336–1342.
85. Dill T, Neumann T, Ekinci O, et al. Pulmonary vein diameter reduction after radiofrequency catheter ablation for paroxysmal atrial fibrillation evaluated by contrast-enhanced three-dimensional magnetic resonance imaging. Circulation 2003;107:845–850.
86. Saad EB, Rossillo A, Saad CP, et al. Pulmonary vein stenosis after radiofrequency ablation of atrial fibrillation: functional characterization, evolution, and influence of the ablation strategy. Circulation 2003;108:3102–3107.
87. Scanavacca MI, D'Avila A, Parga J, Sosa E. Left atrial-esophageal fistula following radiofrequency catheter ablation of atrial fibrillation. J Cardiovasc Electrophysiol 2004;15:960–962.
88. Lemola K, Sneider M, Desjardins B, et al. Computed tomographic analysis of the anatomy of the left atrium and the esophagus: implications for left atrial catheter ablation. Circulation 2004;110:3655–3660.
89. Schaffler GJ, Groell R, Peichel KH, Rienmuller R. Imaging the coronary venous drainage system using electron-beam CT. Surg Radiol Anat 2000;22:35–39.
90. Lesh MD, Van Hare G, Kao AK, Scheinman MM. Radiofrequency catheter ablation for Wolff–Parkinson–White syndrome associated with a coronary sinus diverticulum. Pacing Clin Electrophysiol 1991;14:1479–1484.
91. Shinbane JS, Lesh MD, Stevenson WG, et al. Anatomic and electrophysiologic relation between the coronary sinus and mitral annulus: implications for ablation of left-sided accessory pathways. Am Heart J 1998;135:93–98.
92. Hwang C, Wu TJ, Doshi RN, Peter CT, Chen PS. Vein of marshall cannulation for the analysis of electrical activity in patients with focal atrial fibrillation. Circulation 2000;101:1503–1505.
93. Mochizuki T, Ohtani T, Higashino H, et al. Tricuspid atresia with atrial septal defect, ventricular septal defect, and right ventricular hypoplasia demonstrated by multidetector computed tomography. Circulation 2000;102:E164–165.
94. Skotnicki R, MacMillan RM, Rees MR, et al. Detection of atrial septal defect by contrast-enhanced ultrafast computed tomography. Cathet Cardiovasc Diagn 1986;12:103–106.
95. Garrett JS, Schiller NB, Botvinick EH, Higgins CB, Lipton MJ. Cine-computed tomography of Ebstein anomaly. J Comput Assist Tomogr 1986;10:664–666.
96. Gerber TC, Kuzo RS. Images in cardiovascular medicine. Persistent left superior vena cava demonstrated with multislice spiral computed tomography. Circulation 2002;105:e79.